Design principles for the area density of dimple patterns

Xiaolei Wang[1,2], Jingqiu Wang[1,2], Bo Zhang[1] and Wei Huang[1,2]

Abstract

Increasing interest has been paid to surface texturing in order to improve tribological properties of sliding surfaces. Currently, the patterns of micro-dimples have attracted more attention since such closed texture cells are supposed to generate additional hydrodynamic pressure easily. It has been proven that the area density of the dimple pattern is a critical parameter for hydrodynamic pressure generation. However, the optimal values of area density obtained by theoretical models are usually different to that obtained from experiments, which show material dependence. In order to understand the design principles of the area density for mixed lubrication regime, a brief review on the studies related to the area density issue of dimple patterns is carried out; the phenomena during contacting and sliding are analyzed numerically in this paper. It is found that the stress concentration and deformation will occur on the contacting and sliding area, and influence the tribological properties of the textured surface significantly depending on the area density and material properties. These negative influences should be considered carefully during surface texture design.

Introduction

TRIZ theory, i.e. the theory of inventive problem solving, has been promoted by Genrich Altshuller and his colleagues, who studied about 400,000 technology patents and from them drew out certain regularities and basic patterns of evolution which governed the processes of solving problems, creating new ideas, and innovation.[1]

One of the most popular TRIZ tools is the "40 inventive principles", which consist of a group of generic solutions that solved technical contradictions across many fields.[2] The "40 inventive principles" includes: curvilinearity (instead of using rectilinear forms, use curvilinear ones); asymmetry change (introduce or increase the degree of asymmetry); combining (combine in space); nesting (putting one thing inside another); moving to a new dimension; replace mechanical systems with fields; turn harm to benefits (use harmful factors to achieve a positive effect); changing properties or parameters, etc.

Indeed, the above principles have been fully reflected in the developing progress of surface texture. As an effective approach to improve the tribological properties of sliding surfaces, surface texture has been studied intensively in the last decade. The advanced manufacturing techniques such as laser and reactive etching provide precision and freedom for the fabrication of surface texture. So that, after the successful application of cross-hatch pattern for the cylinder liner of combustion engine, optimizations have been continually conducted through the groove angle, in combination with laser-etched patterns, etc.;[3–5] various types of surface texture, including dimple and pillar patterns with different shapes and internal structures appeared in engineering field;[6–8] instead of uniformly distributed dimples, partial surface texturing was proposed to improve hydrodynamic effect of sliding bearings;[9] dimples with different sizes were combines on the surface to improve both hydrodynamic effect and running-in process of silicon carbide in water lubrication;[10] not only the dimension of surface texture has been expended from millimeter to nanometer scale, but also micro-magnetic field array was added to work together with the geometric structure;[11] inspired by

[1]College of Mechanical and Electrical Engineering, Nanjing University of Aeronautics and Astronautics, Nanjing, People's Republic of China
[2]Jiangsu Key Laboratory of Precision and Micro-Manufacturing Technology, Nanjing, People's Republic of China

Corresponding author:
Xiaolei Wang, College of Mechanical and Electrical Engineering, Nanjing University of Aeronautics and Astronautics, 29# Yudao Street, Nanjing 210016, People's Republic of China.
Email: wxl@nuaa.edu.cn

the surface structure of the toe pads of tree frog and newt, the patterns for high friction was also studied for the potential applications such as active capsule endoscopy;[12,13] and surface texturing has been applied for various materials including the stiff materials such as ceramics and steel, and also relative soft materials such as UHMWPE and PDMS.

In order to obtain desired performance, increasing attentions have been paid to the mechanisms and design principles of surface texture. Usually, for the objective to decrease friction, adhesion and wear of mechanical components, related mechanisms of surface texture include reserving lubricant to prevent seizure, trapping wear debris to decrease further wear, and particularly, providing additional hydrodynamic effect to increase the load-carrying capacity of parallel sliding surfaces, which is regarded as the most dominant effect of surface texture at the conditions of high speed and low load.[14]

By the hydrodynamic mechanism, the micro-irre-gularities on the surface are able to generate additional hydrodynamic pressure to increase the load-carrying capacity of sliding surfaces.[15] In this way, no matter how much the hydrodynamic pressure is generated, it seems surface texture should be always a good approach to enhance the hydrodynamic lubrication to decrease friction and wear of contacting surfaces. However, although there are a lot of documented results reporting that surface texture has reduced friction successfully, the increase of friction and wear also happens at certain circumstances,[16] and possibly not less than the cases of friction and wear reduction at the complicated lubrication conditions, in which contact and deformation take place. That raises the question of if we are familiar to the mechanisms of friction increasing by surface texture? As indicated by the "40 inventive principles" of TRIZ tools, it is necessary to take action to prevent, or reduce harmful effects. Hence, in order to decrease the friction and wear, it is important to understand the mechanisms to increase friction and wear by the surface texture.

Therefore, a brief review is conducted to summarize the theoretical and experimental studies related to the area density of dimple patterns. Then, numerical analysis is carried out to investigate the contact stress on the edge of surface texture and deformation during contact, which always happens in mixed lubrication regime.

The area density of dimple patterns

In the 1960s, Hamilton et al. indicated that the micro-irregularities on the surface are able to generate the additional hydrodynamic pressure to increase the load-carrying capacity of the sliding surfaces. Although new mechanisms such as "inlet suction",[17] boundary conditions related to cavitation,[18–20] and new modeling method[21] are studied continually,

micro-hydrodynamic effect is regarded as the most dominant effect of surface texture at the conditions of high speed and low load.

The patterns of micro-dimples have attracted more attentions since such closed texture cells are supposed to generate hydrodynamic pressure easily.[22] Dimple diameter, depth, and area density are the major parameters of evenly distributed dimple patterns. Many researchers have contributed to the investigation on the influences of the above parameters on friction and load-carrying capacity of sliding surfaces. It is well accepted that the depth-to-diameter ratio is the most important parameter for the load-carrying capacity of parallel sliding surfaces.

According to the theory of Rayleigh step bearing, the load-carrying capacity varies for different h_1/h_0, and achieves its maximum at $h_1/h_0 = 1.866$, where h_1 and h_0 are the inlet film thickness and the outlet film thickness, respectively. So, it is understandable that the dimple depth equivalent to the film thickness could obtain high hydrodynamic pressure.

The area density of micro-dimples is another important parameter. An objective study by orthogonal method indicated that area density is more significant for the tribological performance than the depth or diameter of dimples.[23]

What is the optimal area density for high load-carrying capacity? As early as in 1999, Etsion et al. developed a model for mechanical seals with regular dimple patterns. The simulation results suggested that the preferable percentage of area density is 20%, and above this value the rate of performance improvement becomes small.[24] After that, a series models based on Reynolds equation have been developed. Usually, these analytical models suggested that the area ratio of 20–40% would be preferable since the total hydrodynamic pressure is maximized within this range. These results were obtained from various simulation conditions including water lubricated bearing,[25] air bearing,[26] gas seal,[27] and even for the contact with soft elastic materials.[28]

At the same time, a series experiments were carried out to investigate the effects of micro-dimples on various surfaces including silicon carbide, metals, and elastomer under different lubrication conditions. It is interesting that the optimal values of area density obtained by experiments were usually different to the theoretical results if the objective was to reduce friction by enhancing hydrodynamic effect in mixed lubrication regime.

For the case of self-mated silicon carbide sliding in water, the experiments showed that the laser textured dimple pattern with the low area density of 2.8% had the effect of friction reduction.[29] Further experiments on the dimple patterns fabricated by reactive ion etching were conducted to obtain the effects of multi-parameters of dimple patterns. The results indicated that the hydrodynamic lubrication could be achieved easily, and the load-carrying capacity could be increased

more than two times by the patterns with the optimized parameters of the dimples, which is 4.9% for area density, and 0.01–0.02 for depth-to-diameter ratio.[25]

For the tribo-pairs of metals lubricated by oil, the optimal area density seems to be slightly higher than that for silicon carbide. Several studies under controlled laboratory conditions support that the area density in the range 5–13% is preferable for friction reduction, and the area density of above 20% usually causes friction increasing. The detailed testing conditions and preferable value of the area density are listed in Table 1.

It needs to be noted that the objective of above researches is to obtain low friction by surface texture. If the anti-seizure ability or friction reduction at boundary lubrication condition is the high priority, particularly at starved lubrication condition, high area density may result in good tribological performance even for hard materials.[36–38] For example, the data of laser texturing on metals show that the pattern of dimples (φ90 μm, depth 2–20 μm, 25%) could increase the maximum PV value (load velocity product) of the mechanical seal obviously;[39] and the dimple pattern with the area density of 15% shows an obvious increase of the critical load for SiC sliding in water.[37] This might because that a relative high area density is helpful to retain lubricant.

Ultra-high molecular weight polyethylene (UHMWPE) has been chosen as the material of concave components of Charnley's low frictional torque joint which is famous and widely used in orthopedic surgeries for nearly 50 years. It has proven that the surface texture is effective to decrease the friction between the contact of UHMWPE and steel. However, the tribological performances are different for the cases whether dimples are on the surface of steel or UHMWPE. While the dimples were on the surface of steel, the area density in the range of 5–15% is effective to reduce friction at a light load. If the dimples were fabricated on the surface of UHMWPE, the dimple area density as high as 30% had the effects of both friction and wear reduction

under water lubrication even at a relative high load.[40,41]

The above results raised the question of what the optimal area density would be if the material becomes softer. Hence, an elastomer with low Young's modulus, polydimethylsiloxane (PDMS), was used as the specimen for further study. The lithography and replica processes were used for surface texture fabrication on the surfaces of PDMS. Dimple patterns with a dimple depth of 5 μm, diameters of 50, 100, and 200 μm, and area densities from 2.6% to 40.1% were fabricated. The original surface of PDMS is hydrophobic with the contact angle around 110°. An oxygen plasma treatment was used to hydrophilize the surface of the PDMS. After the treatment, the contact angle could be decreased to the range of 15°–20°. The friction tests of the PDMS disks sliding against a spherical pin were carried out using both water and a glycerol solution for lubrication. It is found the frictional behavior of surface texture is different for the surfaces of PDMS with different wetting properties. For the hydrophobic surface, high area density and a large number of dimples become critical for reducing friction. In this study, the smallest dimples (with a diameter of 50 mm) and highest area density (40.1%) reduced friction the most. But for the hydrophilic surface, the best area density was around 23% in this experimental condition.[42]

Figure 1 is the summary of the above experimental data. The Y coordinate represents the preferable area density of dimple pattern for friction reduction in mixed lubrication regime. The X coordinate represents the contact modulus E^*, which is defined as

$$\frac{1}{E^*} = \frac{1 - v_1^2}{E_1} + \frac{1 - v_2^2}{E_2}$$

where E_1, E_2 are the Young's modulus, v_1, v_2 are the Poisson's ratio of each side of the tribo-pair, respectively. It could be found that along the decrease of the contact modulus E^*, the dimple patterns with high

Table 1. Testing conditions and preferred values of the area density for metals.

Author/Year	Testing condition	Area density, r		References
		Friction reduction	Friction increase	
Ryk/2002	Ring/liner reciprocating	13%		30
Kovalchenko/2004	52100 Pin/H-13 disk	12%	30%, 40%	31
Kovalchenko/2005	52100 Pin/H-13 disk	7%, 12%		32
Costa/2007	Steel cylinder/plane reciprocating	11%		33
Galda/2009	Ring/block	10%, 12.5%	20%	34
Yan/2010	Ring/disk	5%, 10%	20%	23
Grabon/2013	Ring/cylinder	13%		35

area density could be designed for the surfaces to obtain low friction in mixed lubrication regime.

What are the reasons for the difference between analytical and experimental results? It is obvious that the most theoretical models only consider the hydrodynamic effect while the experiments usually can not avoid contact between two surfaces. Therefore, the contact problem including contact stress and deformation will be analyzed in the following parts.
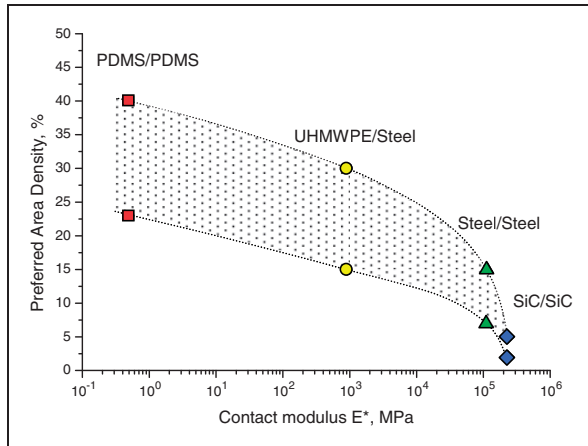

Figure 1. Preferable area density of dimple patterns for different materials.

The contact stress at the edges of surface texture

For the surfaces sliding in mixed lubrication regime, there is always a portion of area contacting in solid. Hence, the geometric contour of surface texture would definitely influence the contact pressure distribution between surfaces.

An finite element method (FEM) analysis was carried out to simulate the contact situation of the edges of surface texture during sliding.[43] Figure 2 shows both the model and the simulation results. The contact problem was simplified as a block sliding against a plane surface with contact. So the two edges of the block are perpendicular and parallel to the sliding direction, respectively. The width and length of the upper block are 0.1 mm, and the height of the block is 0.02 mm. Both contacting surfaces are smooth ignoring surface roughness. The element "structural" was used and the simulation conditions are listed in Table 2.

The colors on the upper block represent von Mises stress obtained by the simulation. It is obvious that there is relatively high stress at the edge while it is perpendicular to the sliding direction. Comparatively, there is almost no stress while the edge is parallel to the sliding direction. The edge stresses should be caused by not only the stress discontinuity because of sharp changes in profile but also the motion of
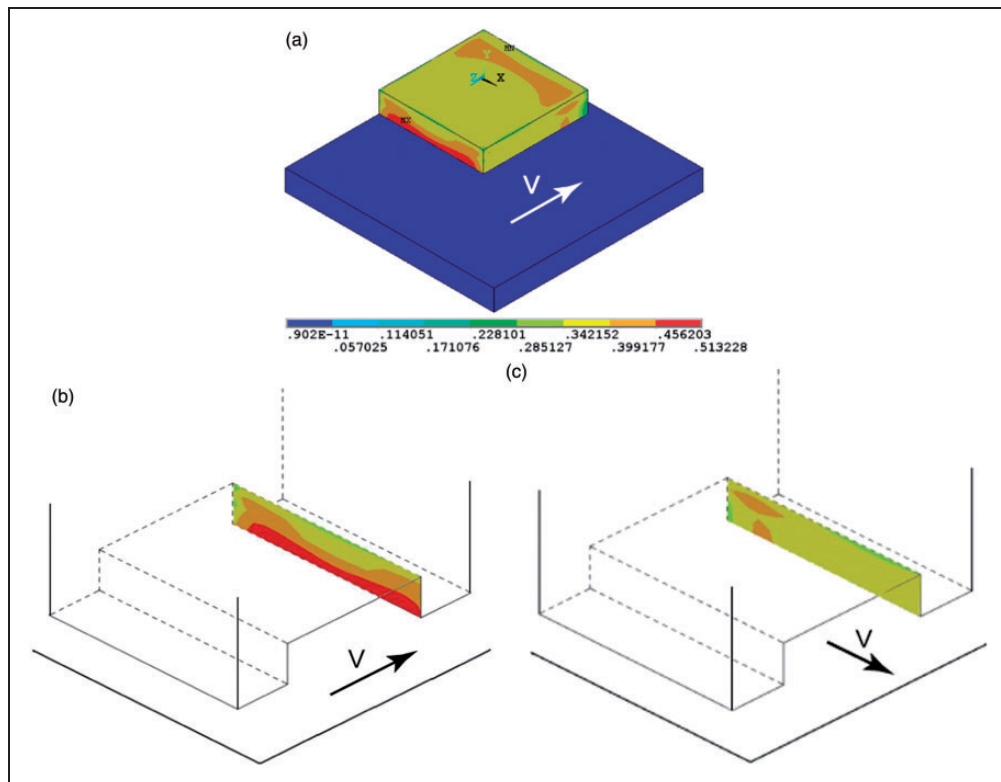

Figure 2. Contacting stress at the edges with different sliding directions.

sliding. Therefore, as illustrated in Figure 2(b) and (c), if there are grooves on the contacting surface, the stress is different depending on whether the groove is parallel or perpendicular to the sliding direction. For same reason, the contact stress at the edge of a dimple would also depend on its relationship to sliding direction. This phenomenon needs to be noted particularly while the shape of the dimples is not circular.

Next question is whether there is any difference for fabricating the surface texture on a stiff or a soft material. A simulation by the FEM software ANSYS was carried out to investigate the stress distribution around the edge of a dimple.[40] The contact problem was simplified as a dimpled block sliding against a plane surface with contact. The size of the dimple is 50 μm in diameter. Both contacting surfaces are smooth, ignoring surface roughness. SiC was selected as the stiff materials, UHMWPE as the relative soft material, for texturing, and sliding against the same material, SUS 316 stainless steel.

The element "structural" was used and simulation conditions are listed in Table 3.

Figure 3 presents the contact stress distribution around the dimple. Figure 3(a) shows the results of dimpled SiC contacting and sliding against SUS 316, and Figure 3(b) is the case of dimpled UHMWPE sliding against SUS 316. Clearly, although the average contact pressures are the same, the stress is concentrate along the edge of the dimple for the stiff material SiC, as well as the stress relatively spread over the whole contacting surface for the case of UHMWPE.
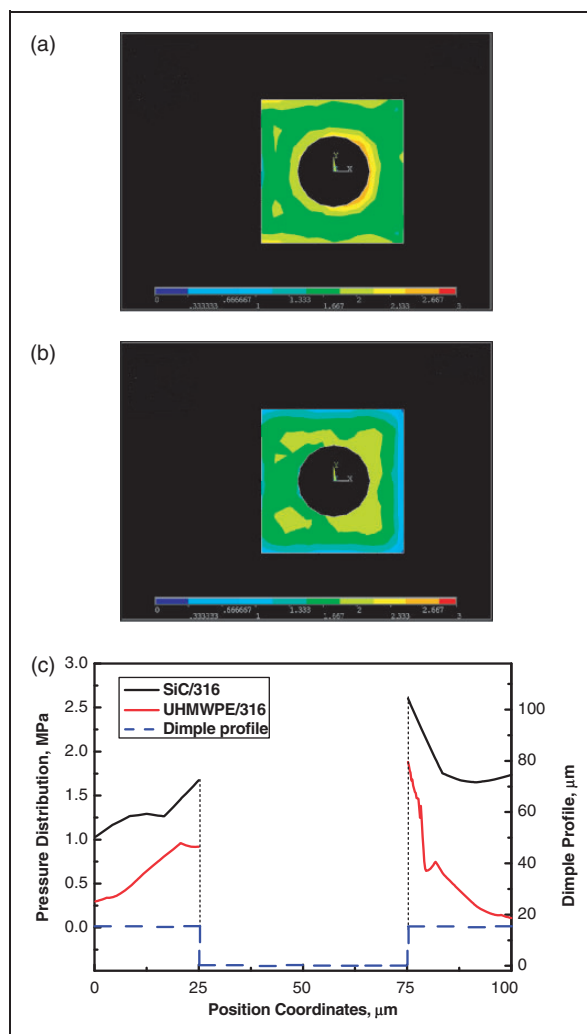
Figure 3(c) shows the stress profile along the horizontal central line of the dimple. It is obvious that stress at the edge of SiC is higher than that of UHMWPE although their average contact pressures are the same. For the same surface, the stress at the edge of converging side is higher than that at the edge of diverging side due to the motion of sliding. The difference for the highest stress is larger than 50% in this simulation condition. If the average contact pressure is increased, the difference of stress will also increase. High contact stress will induce large deformation at specific locations, i.e. the area contacted by the edge of dimple in this case, which results in the increase of overall friction force. That may be the reason that usually the ultra-smooth surface is used for current design of artificial joint.

Table 2. Simulation conditions for the block sliding against a plane surface.

Contact pressure, $P = 0.5$ MPa
Young's modulus, $E = 120$ GPa
Poisson's ratio, $\nu = 0.25$
Friction coefficient, $\mu = 0.10$
Sliding velocity, $V = 0.1$ mm/s

Table 3. Simulation conditions for the dimpled block sliding against a plane surface.

Contact pressure, $P = 1.67$ MPa
Young's modulus of SiC, $E_1 = 450$ GPa
Young's modulus of UHMWPE, $E_2 = 0.69$ GPa
Young's modulus of 316 steel, $E_3 = 199$ GPa
Poisson's ratio of SiC, $\nu_1 = 0.14$
Poisson's ratio of UHMWPE, $\nu_2 = 0.49$
Poisson's ratio of SUS 316, $\nu_3 = 0.26$
Friction coefficient, $\mu = 0.10$
Area density, $r = 20\%$
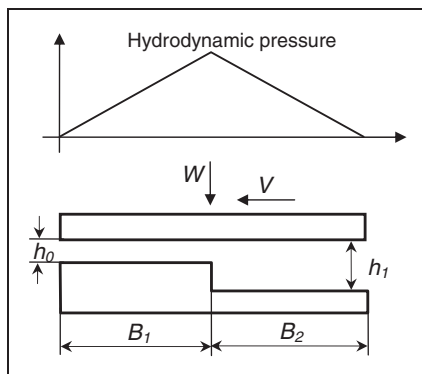Sliding velocity, $V = 0.1$ mm/s

Figure 3. Pressure distribution around a dimple: (a) dimpled SiC/SUS316; (b) dimpled UHMWPE/SUS316; (c) pressure profile along the horizontal central line of the dimple.

Therefore, if the dimple is fabricated on the stiff material, higher stress will generated on the edge perpendicular to the sliding direction. And higher area density means there are more high stressed area, which is critical for stiff materials. This stress will definitely results in deformation, energy consumption, which will finally cause a friction increase, particularly when the contact pressure is high. Therefore, the optimal value of the area density obtained by experiment is usually lower than that by the theoretical analysis only based on Reynolds equation, and the optimal value of the area density for ceramics is lower than that for metals and polymers.

Surface texture induced deformation

The load-carrying capacity could be increased by the dimples on the surface, which are considered as micro-step bearings. As shown in Figure 4, in a Rayleigh step bearing, the load-carrying capacity varies for different h_1/h_0, and achieves its maximum at $h_1/h_0 = 1.866$, where h_1 and h_0 are the inlet film thickness and the outlet film thickness, respectively. By a relative sliding, the hydrodynamic pressure will be generated and distribute as a triangle shown in Figure 4, at which the highest pressure will be at the edge of the step. Yagi and Sugimura[44] conducted an elastohydrodynamic numerical simulation for one-dimensional Rayleigh step bearings made of steel. It is found that a small elastic deformation of less than 200 nm is responsible for film formation in thin film hydrodynamic lubrication. As the film thickness decreases to the scale of sub-micro meter, the divergent shape in the step zone causes delay in pressure growth, resulting in considerable reduction of load capacity while the convergent shape in the land zone improves slightly load capacity in some cases.

The deformation would be more obvious if the step side is made of a softer material. It will influence the pressure distribution even while the film thickness is

relative thick. Figure 5(a) is a simple simulation result showing the deformation of PDMS caused by hydrodynamic pressure. The simulation conditions are listed in Table 4.

By a set of optimized parameters, $h_0 = 3\,\mu m$, $h_1 = 5.6\,\mu m$, $B_1 = 2\,mm$, $B_2 = 2\,mm$, without considering the deformation, the highest pressure at the edge of the step can be obtained as shown in Figure 5(b).

By the hydrodynamic pressure, the step side made of low Young's modulus material will be pressed to form a deformation. The dot line in Figure 5(a) shows original shape of the step, while the colored area
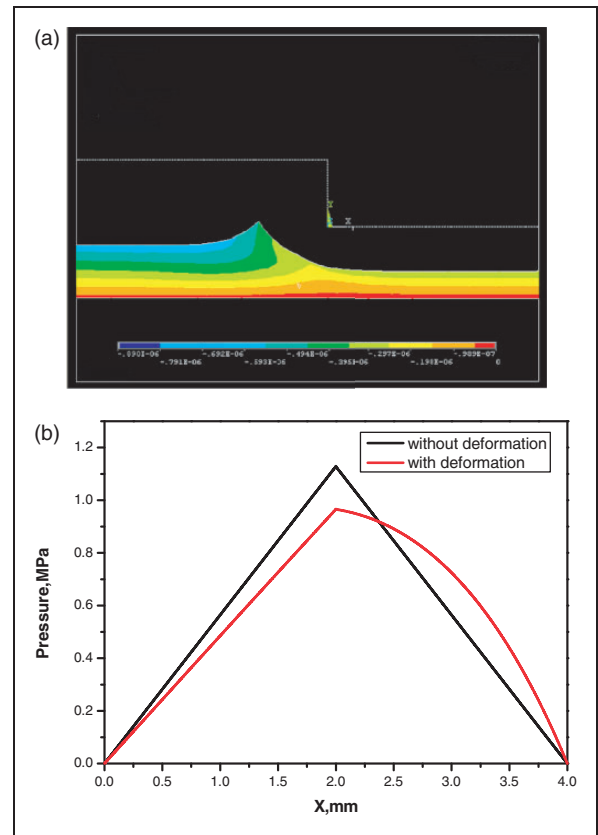
Figure 5. Deformation and the change of hydrodynamic pressure occurred on the step made of PDMS: (a) the shape of the step before and after the deformation; (b) the hydrodynamic pressure distribution before and after the deformation.

Figure 4. A Rayleigh step bearing and the pressure distribution.

Table 4. Simulation conditions for the deformation of PDMS.

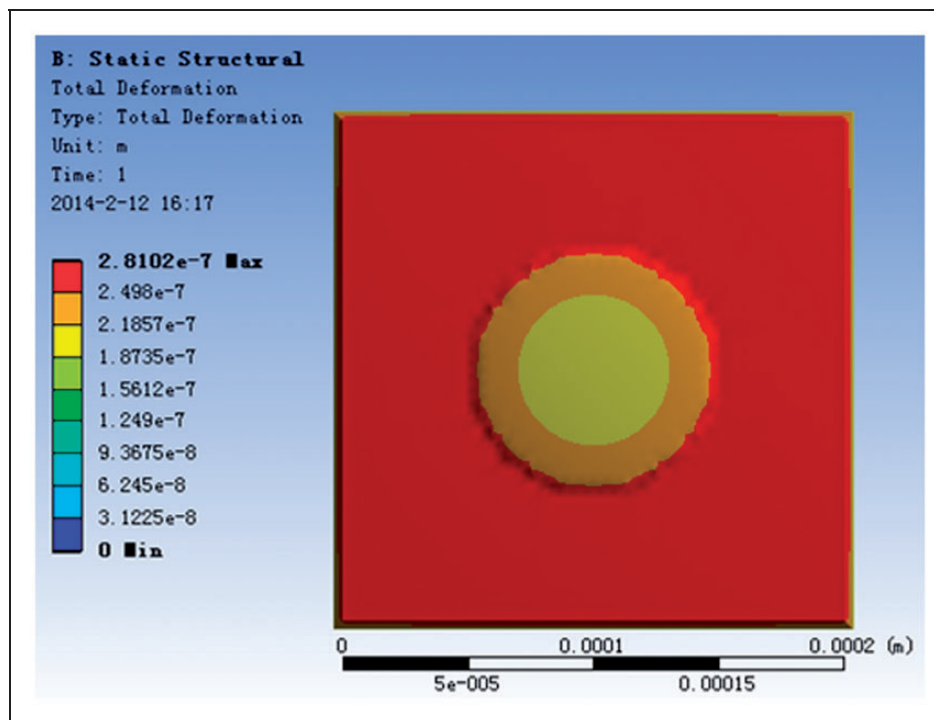| |
|---|
| Material of step side: PDMS |
| Young's modulus of PDMS, $E_1 = 750\,kPa$ |
| Poisson's ratio of PDMS, $\nu_1 = 0.5$ |
| Sliding velocity, $V = 0.5\,m/s$ |
| The plain side is rigid, ignoring deformation. |

PDMS: polydimethylsiloxane.

Figure 6. Deformation of UHMWPE while it contacts with a dimpled stainless steel.

shows the shape after deformation. The colors present the displacements of the materials. It could be found the maximum deformation will be near 3 μm under above condition if the change of hydrodynamic pressure were ignored. This deformation changes the shape of the step bearing greatly. Fortunately, the converging wedge is still there, so that the hydrodynamic pressure is still generated. But definitely, the step bearing will lose it optimized parameter. Both the maximum pressure and the load-carrying capacity decrease as shown in Figure 5(b). Of course, it is just a simple simulation ignoring the change of pressure during the deformation. On the other hand, for the possibility that the hydrodynamic pressure and load-carrying capacity are increased after deformation, it needs further study considering mutual influence of hydrodynamic pressure and the deformation. Another problem is the leakage, caused by deformation while regional pressure becomes high enough. These are the reasons that stiff bearings usually offering theoretically greater load-bearing capacity than comparable elastic bearings.

Figure 6 shows the simulation results of a dimpled stainless steel 316 contacted with a plane surface of UHMWPE by the elements of "fluent" and "structural". By the contact pressure of 1.67 MPa, the contacting surface of UHMWPE would be pressed, while the surface inside of the dimple will "swell up" relatively. The difference of the height inside and outside the dimple will be up to 0.1–0.2 μm in this simulation condition. Therefore, if the stiff surface slides against the soft surface with relative high contact pressure, the

continuous deformation on the soft material will consume energy, result in friction increase. More seriously, if the dimple edge on the stiff material is sharp enough and the deformation is large enough, the cutting wear will happen easily. Therefore, the experimental results show that the preferable area density for stiff material could not be as high as that for soft materials.

Summary

As an effective approach, surface texture provides various ways to improve the tribological properties of sliding surfaces. Although the design principle of dimple patterns following hydrodynamic theory has been well accepted, experimental and analytical studies carried out by different researchers suggest that in order to obtain desirable tribological performance, the surface texture design needs to be conducted according to the type of contact, materials of the tribo-pair, and operating conditions.

Area density is an important parameter in dimple pattern design. Theoretical models based on hydrodynamic principles usually suggest a relative high area density to maximize the load-carrying capacity. However, in the mixed lubrication regime with high contact pressure, the stress concentration at the edges of surface texture need to be carefully considered, particularly, for the case while the texture is fabricated on the stiff material with high area density.

For the tribo-pairs with relative soft materials, deformation happened on the soft material. It needs to be further studied since deformation will influence

the hydrodynamic pressure distribution, also may induce cutting wear on the soft material.

Conflict of interest

None declared.

References

1. Ilevbare IM, Probert D and Phaal R. A review of TRIZ, and its benefits and challenges in practice. *Technovation* 2013; 33(2–3): 30–37.
2. Petković D, Issa M, Pavlović ND, et al. Application of the TRIZ creativity enhancement approach to design of passively compliant robotic joint. *Int J Adv Manuf Technol* 2012; 67(1–4): 865–875.
3. Michail SK and Barber GC. The effects of roughness on piston ring lubrication—Part II: The relationship between cylinder wall surface topography and oil film thickness. *Tribol Trans* 1995; 38(1): 173–177.
4. Spencer A, Almqvist A and Larsson R. A semi-deterministic texture-roughness model of the piston ring-cylinder liner contact. *Proc IMechE, Part J: J Engineering Tribology* 2011; 225(6): 325–333.
5. Rahnejat H, Balakrishnan S, King PD, et al. In-cylinder friction reduction using a surface finish optimization technique. *Proc IMechE, Part D: J Automobile Engineering* 2006; 220(9): 1309–1318.
6. Stephens LS, Siripuram R, Hayden M, et al. Deterministic micro asperities on bearings and seals using a modified LIGA process. *J Eng Gas Turbines Power* 2004; 126: 147–154.
7. Yu H, Wang X and Zhou F. Geometric shape effects of surface texture on the generation of hydrodynamic pressure between conformal contacting surfaces. *Tribol Lett* 2010; 37(2): 123–130.
8. Shen C and Khonsari MM. Effect of dimple's internal structure on hydrodynamic lubrication. *Tribol Lett* 2013; 52(3): 415–430.
9. Brizmer V, Kligerman Y and Etsion I. A laser surface textured parallel thrust bearing. *Tribol Trans* 2003; 46(3): 397–403.
10. Wang XL, Adachi K, Otsuka K, et al. Optimization of the surface texture for silicon carbide sliding in water. *Appl Surf Sci* 2006; 253(3): 1282–1286.
11. Shen C, Huang W, Ma GL, et al. A novel surface texture for magnetic fluid lubrication. *Surf Coat Technol* 2009; 204(4): 433–439.
12. Huang W and Wang X. Biomimetic design of elastomer surface pattern for friction control under wet conditions. *Bioinspir Biomim* 2013; 8(4): 046001.
13. Buselli E, Pensabene V, Castrataro P, et al. Evaluation of friction enhancement through soft polymer micro-patterns in active capsule endoscopy. *Meas Sci Technol* 2010; 21(10): 105802.
14. Yu H, Huang W and Wang X. Dimple patterns design for different circumstances. *Lubric Sci* 2013; 25: 67–78.

15. Hamilton DB, Walowit JA and Allen CM. A theory of lubrication by micro-irregularities. *J Basic Eng* 1966; 88(1): 177–185.
16. Qiu Y and Khonsari MM. Experimental investigation of tribological performance of laser textured stainless steel rings. *Tribol Int* 2011; 44(5): 635–644.
17. Fowell M, Olver AV, Gosman AD, et al. Entrainment and inlet suction: Two mechanisms of hydrodynamic lubrication in textured bearings. *J Tribol* 2007; 129: 336–347.
18. Brajdic-Mitidieri P, Gosman AD, Ioannides E, et al. CFD analysis of a low friction pocketed pad bearing. *J Tribol Trans ASME* 2005; 127(4): 803–812.
19. Shen C and Khonsari MM. On the magnitude of cavitation pressure of steady-state lubrication. *Tribol Lett* 2013; 51(1): 153–160.
20. Zhang J and Meng Y. Direct observation of cavitation phenomenon and hydrodynamic lubrication analysis of textured surfaces. *Tribol Lett* 2012; 46(2): 147–158.
21. Han J, Fang L, Sun J, et al. Hydrodynamic lubrication of microdimple textured surface using three-dimensional CFD. *Tribol Trans* 2010; 53(6): 860–870.
22. Nakano M, Korenaga A, Korenaga A, et al. Applying micro-texture to cast iron surfaces to reduce the friction coefficient under lubricated conditions. *Tribol Lett* 2007; 28: 131–137.
23. Yan D, Qu N, Li H, et al. Significance of dimple parameters on the friction of sliding surfaces investigated by orthogonal experiments. *Tribol Trans* 2010; 53(5): 703–712.
24. Etsion I and Burstein L. A model for mechanical seals with regular microsurface structure. *Tribol Trans* 1996; 39(3): 677–683.
25. Wang XL, Kato K, Adachi K, et al. Loads carrying capacity map for the surface texture design of SiC thrust bearing sliding in water. *Tribol Int* 2003; 36(3): 189–197.
26. Murthy AN, Etsion I and Talke FE. Analysis of surface textured air bearing sliders with rarefaction effects. *Tribol Lett* 2007; 28: 251–261.
27. Kligerman Y and Etsion I. Analysis of the hydrodynamic effects in a surface textured circumferential gas seal. *Tribol Trans* 2001; 44(3): 472–478.
28. Shinkarenko A, Kligerman Y and Etsion I. The effect of surface texturing in soft elasto-hydrodynamic lubrication. *Tribol Int* 2009; 42(2): 284–292.
29. Wang XL, Kato K, Adachi K, et al. The effect of laser texturing of SiC surface on the critical load for transition of water lubrication mode from hydrodynamic to mixed. *Tribol Int* 2001; 34(10): 703–711.
30. Ryk G, Kligerman Y and Etsion I. Experimental investigation of laser surface texturing for reciprocating automotive components. *Tribol Trans* 2002; 45(4): 444–449.
31. Kovalchenko A, Ajayi O, Erdemir A, et al. The effect of laser texturing of steel surfaces and speed-load parameters on the transition of lubrication regime from boundary to hydrodynamic. *Tribol Trans* 2004; 47(2): 299–307.
32. Kovalchenko A, Ajayi O, Erdemir A, et al. The effect of laser surface texturing on transitions in lubrication regimes during unidirectional sliding contact. *Tribol Int* 2005; 38(3): 219–225.

33. Costa HL and Hutchings IM. Hydrodynamic lubrication of textured steel surfaces under reciprocating sliding conditions. *Tribol Int* 2007; 40(8): 1227–1238.

34. Galda L, Pawlus P and Sep J. Dimples shape and distribution effect on characteristics of Stribeck curve. *Tribol Int* 2009; 42(10): 1505–1512.

35. Grabon W, Koszela W, Pawlus P, et al. Improving tribological behaviour of piston ring–cylinder liner frictional pair by liner surface texturing. *Tribol Int* 2013; 61: 102–108.

36. Wang XL, Kato K and Adachi K. The lubrication effect of micro-pits on parallel sliding faces of SiC in water. *Tribol Trans* 2002; 45(3): 294–301.

37. Wang XL and Kato K. Improving the anti-seizure ability of SiC seal in water with RIE texturing. *Tribol Lett* 2003; 14(4): 275–280.

38. Zum Gahr KH, Mathieu M and Brylka B. Friction control by surface engineering of ceramic sliding pairs in water. *Wear* 2007; 263(7–12): 920–929.

39. Halperin G, Greenberg Y and Etsion I. Increasing mechanical seals life with laser-textured seal faces. In: *Proceedings of the 15th International Conference on Fluid Sealing-BHR Group*, Maastricht, 1997, pp.3–11.

40. Zhang B, Huang W and Wang X. Biomimetic surface design for ultrahigh molecular weight polyethylene to improve the tribological properties. *Proc IMechE, Part J: J Engineering Tribology* 2012; 226(8): 705–713.

41. Zhang B, Huang W, Wang J, et al. Comparison of the effects of surface texture on the surfaces of steel and UHMWPE. *Tribol Int* 2013; 65: 138–145.

42. Huang W, Jiang L, Zhou C, et al. The lubricant retaining effect of micro-dimples on the sliding surface of PDMS. *Tribol Int* 2012; 52: 87–93.

43. Yuan S, Huang W and Wang X. Orientation effects of micro-grooves on sliding surfaces. *Tribol Int* 2011; 44(9): 1047–1054.

44. Yagi K and Sugimura J. Elastohydrodynamic simulation of Rayleigh step bearings in thin film hydrodynamic lubrication. *Tribol Int* 2013; 64: 204–214.

Appendix

Notation

B_1, B_2	length
E, E_1, E_2, E_3	Young's modulus (GPa)
E^*	contact modulus (MPa)
h_0	outlet film thickness (µm)
h_1	inlet film thickness (µm)
P	contact pressure (MPa)
r	area density (%)
V	sliding velocity
W	load
μ	friction coefficient
ν, ν_1, ν_2	Poisson's ratio